PROTEINS
STRUCTURE ■ FUNCTION ■ BIOINFORMATICS

Engineering proteins with tunable thermodynamic and kinetic stabilities

Angel L. Pey, David Rodriguez-Larrea, Susanne Bomke, Susanne Dammers, Raquel Godoy-Ruiz, Maria M. Garcia-Mira, and Jose M. Sanchez-Ruiz*

Departamento de Quimica Fisica, Facultad de Ciencias, Universidad de Granada, 18071-Granada, Spain

ABSTRACT

It is widely recognized that enhancement of protein stability is an important biotechnological goal. However, some applications at least, could actually benefit from stability being strongly dependent on a suitable environment variable, in such a way that enhanced stability or decreased stability could be realized as required. In therapeutic applications, for instance, a long shelf-life under storage conditions may be convenient, but a sufficiently fast degradation of the protein after it has performed the planned molecular task in vivo may avoid side effects and toxicity. Undesirable effects associated to high stability are also likely to occur in food-industry applications. Clearly, one fundamental factor involved here is the kinetic stability of the protein, which relates to the time-scale of the irreversible denaturation processes and which is determined to some significant extent by the free-energy barrier for unfolding (the barrier that "separates" the native state from the highly-susceptible-to-irreversible-alterations nonnative states). With an appropriate experimental model, we show that strong environment-dependencies of the thermodynamic and kinetic stabilities can be achieved using robust protein engineering. We use sequence-alignment analysis and simple computational electrostatics to design stabilizing and destabilizing mutations, the latter introducing interactions between like charges which are screened out at high salt. Our design procedures lead naturally to mutating regions which are mostly unstructured in the transition state for unfolding. As a result, the large salt effect on the thermodynamic stability of our consensus plus charge-reversal variant translates into dramatic changes in the time-scale associated to the unfolding barrier: from the order of years at high salt to the order of days at low salt. Certainly, large changes in salt concentration are not expected to occur in biological systems in vivo. Hence, proteins with strong salt-dependencies of the thermodynamic and kinetic stabilities are more likely to be of use in those cases in which high-stability is required only under storage conditions. A plausible scenario is that inclusion of high salt in liquid formulations will contribute to a long protein shelf-life, while the lower salt concentration under the conditions of the application will help prevent the side effects associated with high-stability which may potentially arise in some therapeutic and food-industry applications. From a more general viewpoint, this work shows that consensus engineering and electrostatic engineering can be readily combined and clarifies relevant aspects of the relation between thermodynamic stability and kinetic stability in proteins.

Proteins 2008; 71:165–174.

Key words: protein stability; kinetic stability; free-energy barriers; salt effects.

INTRODUCTION

It is widely recognized that enhancement of protein stability is convenient or even essential for many technological and therapeutical applications of proteins. Significant success in obtaining protein variants of enhanced stability has been achieved on the basis of rational/computational methodologies,[1–5] sequence-alignment analysis,[6–9] and *in vitro* directed evolution.[10] However, one relevant point has received little attention: in some cases at least, stability enhancement may be required only under specific conditions. For instance, therapeutic applications of proteins should benefit from an enhanced stability of the protein-drug under storage conditions (as reflected in a sufficiently long shelf-life), but this same high-stability may be undesirable under the conditions of the application *in vivo*,

The Supplementary Material referred to in this article can be found online at http://www.interscience.wiley.com/jpages/0887-3585/suppmat/
Grant sponsor: Spanish Ministry of Education and Science; Grant number: BIO2006-07332; Grant sponsor: FEDER; Grant sponsor: Junta de Andalucia; Grant number: CVI-771.
A. L. Pey's current address is Department of Biomedicine, University of Bergen, Jonas Lies vei 91, N-5009 Bergen, Norway.
*Correspondence to: Jose M. Sanchez-Ruiz, Facultad de Ciencias, Departamento de Quimica Fisica, Fuentenueva s/n, 18071-Granada, Spain. E-mail: sanchezr@ugr.es
Received 22 March 2007; Revised 29 May 2007; Accepted 11 June 2007
Published online 11 October 2007 in Wiley InterScience (www.interscience.wiley.com). DOI: 10.1002/prot.21670

since it may lead to slow degradation and, consequently, to side effects and toxicity. A ribonuclease from *Rana pipiens* oocytes and embryos, usually known as onconase, provides a clear example of this situation. This protein has been shown to be specifically cytotoxic for some types of cancer cells.[11] This activity is higher than that of other ribonucleases and, in fact, onconase is currently at phase III clinical trials with humans for the treatment of some types of cancer. The main side effect of onconase, after its administration, is its renal toxicity,[12,13] which appears to be associated to its slow degradation and, ultimately, to the unusually high stability of this enzyme, much higher in fact than that of other ribonucleases.[14] Undesirable effects associated to high stability are also likely to occur in food-industry applications.

It appears, therefore, that many applications of proteins could actually benefit from stability being strongly dependent of a suitable environment variable, in such a way that enhanced stability or decreased stability could be realized as required (for instance, enhanced stability under storage conditions and decreased stability under the actual conditions of the application). Here we use a convenient experimental model (*Escherichia coli* thioredoxin) to show how this feature can be implemented using robust and widely-applicable protein engineering. We use the salt concentration as an easily-controllable environment variable and our approach is based on the introduction of both stabilizing and destabilizing mutations, with the latter involving interactions between charges of the same sign which are screened out at high salt concentration. This certainly produces the desired environment-dependence of the thermodynamic stability (enhanced stability at high-salt and decreased stability at low-salt).

It is very important to note, however, that thermodynamic stability (as measured by the unfolding free-energy change or by the equilibrium denaturation temperature) may not be the critical factor for many applications of proteins[15]; actually, it may not even be the most important factor determining protein stability *in vivo*.[16] What is relevant in many cases is actually the *kinetic* stability of the protein, which relates more directly with practical parameters of interest, such as shelf-life, half-life time for degradation, and so forth. Kinetic stability can be described in terms of the rate of irreversible protein denaturation and is often discussed on the basis of simple Lumry–Eyring models,[16–19] such as:

$$\text{Native state} \Leftrightarrow \text{Nonnative ensemble} \rightarrow \text{Irreversible denatured protein} \quad (1)$$

where the nonnative ensemble is defined to include unfolded and partially-unfolded states. Irreversible alterations of protein states occur both *in vitro* and *in vivo* (aggregation, chemical modification of residues, interactions with other macromolecular components, proteolysis, etc.). Lumry–Eyring models are consistent with the known experimental fact that thermodynamic stability does not guarantee that the protein will remain in the native state during a given time-scale, since irreversible alterations (even if they occur from lowly populated unfolded or partially unfolded states) may deplete the native state in a time-dependent manner.[16–19] Furthermore, simple Lumry–Eyring models [such as Eq. (1)] emphasize the significant role of the unfolding free-energy barrier (the barrier that "separates" the native state from the nonnative ensemble) in determining kinetic stability. As we have recently noted,[20] this role is twofold: (a) if irreversible alterations occur mainly from nonnative states, the overall irreversible process cannot be faster than the rate of unfolding[16]; (b) for a high unfolding barrier, the states that "form" the barrier have high free-energy and are not significantly populated; as a result, irreversible alteration processes that occur from those states are disfavored.[21,22] Thus, a sufficiently high unfolding free-energy barrier provides a "safety mechanism" that favors significant kinetic stability even in an aggressive environment; conversely, a low unfolding free-energy barrier implies that efficient pathways for irreversible denaturation may be operative in many environments. Indeed, many studies are consistent with a significant role of the unfolded free-energy barrier in kinetic stability. For instance, kinetic analyses of irreversible thermal denaturation of proteins suggest that the unfolding barrier limits the overall rate of the process.[16,19] Also, a slow unfolding rate is often observed in proteins from hyperthermophilic organisms[23–25] and high unfolding barriers have been found in kinetically stable extracellular bacterial proteases.[26] Finally, in a very recent work,[27] Marqusee and coworkers have proteolitically challenged the proteome of *E. coli* and found a surprisingly large number of proteins resistant to proteolysis. In order to determine the general origin of such resistance, these authors analyzed in detail the case of the maltose binding protein and found that its resistance to thermolysin degradation was indeed due to high kinetic stability associated to a very large unfolding free-energy barrier.

In order for mutation effects on thermodynamic stability to be fully "transmitted" to the unfolding free-energy barrier, mutations must be carried in regions of the protein which are "nonstructured" in the unfolding transition state. As we expound in detail in the Results and Discussion section, the design approaches we have used lead naturally to mutations fulfilling this criterion. Accordingly, our designed large salt-dependence of thermodynamic stability translates into a similarly large salt effect on the unfolding rates.

One final important point must be made: when dealing with kinetic processes involving proteins (folding/unfolding kinetics, irreversible denaturation, shelf-life, etc.), the most fundamental phenomenological feature one would like to predict/control is actually the time-scale (years?, months?, days?, hours? . . . milliseconds?, microseconds? . . .).

As we have recently emphasized,[20] the half-life time of a barrier-limited kinetic process changes in an exponential manner with the activation free-energy and, consequently, even moderate free-energy changes in barrier height produce dramatic effects in the time-scale of the process. Indeed, we find huge salt effects on the time-scale for the unfolding of our designed multiple-mutant variant of thioredoxin, which is estimated to be on the order of years at high-salt and on the order of days at low-salt. Obviously, such a huge effect on time-scale should also hold for any process (irreversible denaturation occurring from nonnative states) which is limited by the "crossing" of the same unfolding free-energy barrier.

METHODS

Sequence alignments

The sequence alignment used has been previously described and published.[28] Briefly, BLAST 2 [Gish W (1996–2003) http://blast.wust1.edu] was used to search the UniProt/TrEMBL database with the sequence of *E. coli* thioredoxin as query and the default options of the search. The sequences found were aligned to the query sequence using the Smith–Waterman algorithm and those with sequence identity with the query higher than 0.25 were retained. Out of the 491 sequences selected in this way, 100 belonged to proteobacteria. These 100 sequences were used to calculate the ratios of frequencies of occurrence given in Figure 1(A).

Computational electrostatics

Electrostatic calculations were performed using the Tanford–Kirkwood model with the Gurd correction, as we have previously described in detail.[29] This simple model neglects solvation effects and only takes into account charge–charge interactions. This is very convenient for our purposes, since we are interested in the electrostatic interactions which are susceptible to be screened by salt.

Mutagenesis, expression, purification, and activity of the thioredoxin variants

Preparation of wt and variant forms of *E. coli* thioredoxin was carried out as previously described,[30,31]

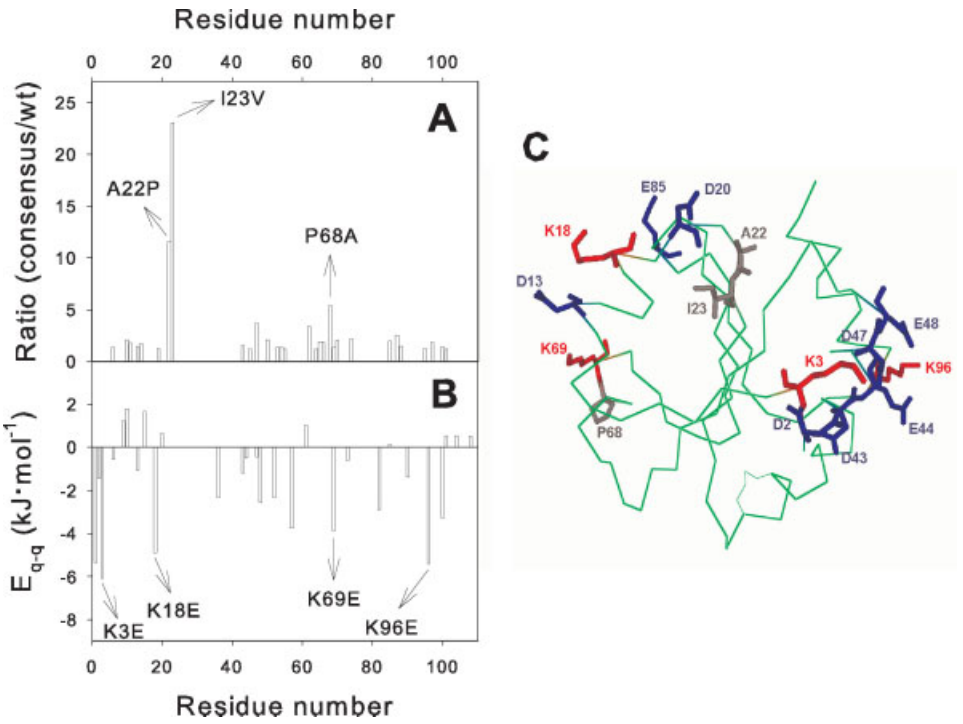

Figure 1

Designing stabilizing and destabilizing mutations in E. coli *thioredoxin. (**A**) Consensus design of stabilizing mutations. The wt sequence is compared with the consensus sequence derived from the proteobacteria sequences obtained from a BLAST search of the UniProt/TrEMBL database using the sequence of* E. coli *thioredoxin as query. In those positions in which the consensus residue differs from the wt residue, the ratio of the corresponding frequencies in the set of proteobacteria sequences is given. The three highest values for this ratio are labelled with the suggested wt→consensus mutation. (**B**) Electrostatic design of destabilizing mutations. A simple Tanford–Kirkwood algorithm is used to calculate the energies of charge–charge interactions for all charged residues in the thioredoxin molecule. The four largest negative values are labelled with the suggested charge reversal mutations. (**C**) Thioredoxin structure showing the residues to be mutated according to the calculations shown in panels (A) and (B). For illustration, we also show some carboxylic acid residues close to the lysine residues to be mutated.*

except that we used the plasmid pET30a (into which the thioredoxin gene had been subcloned) and BL21(DE3) supercompetent cells for overexpression. Enzyme activity of wt thioredoxin, the consensus V3 variant and consensus *plus* charge-reversal V6 variant (see Results and Discussion for a description of these variants) was determined using two different procedures (see supplementary Fig. 1S): (1) A turbidimetric assay of the thioredoxin-catalyzed rate of reduction of insulin[32]; (2) a coupled assay with thioredoxin reductase using DTNB as electron acceptor.[33] The three forms showed essentially the same activity in the insulin reduction assay. The coupled assay with thioredoxin reductase gave an activity for the V3 and V6 variants of about 56% and 21% of that for the WT protein.

Differential scanning calorimetry

Differential scanning calorimetry (DSC) experiments were carried out using a capillary VP-DSC microcalorimeter from MicroCal (Northhampton, USA) equipped with the autosampler attachment. Cell volume in this instrument is 0.135 mL. Protein solutions for DSC experiments were prepared by exhaustive dialysis against the buffer (5 m*M* Hepes, pH7). For experiments in the presence of urea, guanidine, and NaCl, adequate amounts of stock solutions in the same buffer were added. Protein concentrations were determined from the absorbance at 280 nm, and guanidine and urea concentrations from refraction index measurements. NaCl concentrations were determined by weight. All experiments were carried out at a scan rate of 2.5°/min and under an overpressure of 4 bar to prevent degassing during the scan and increase the boiling point so that scans can proceed up to 120°. In all cases, the DSC transitions were found to be reversible in a second heating run and to be adequately described by the two-state equilibrium model. Values of the equilibrium denaturation temperature (T_m) and the unfolding enthalpy at the T_m were derived from these fits.

Folding/unfolding kinetics followed by fluorescence

Folding/unfolding kinetics at 25° in 5 m*M* Hepes, pH 7, were monitored by following the time-dependence of the fluorescence emission at 350 nm (excitation at 276 nm) after suitable urea or guanidine concentration jumps. Apparent, folding/unfolding rate constants (k) were calculated from the fittings of a first-order rate equation to the experimental fluorescence intensity versus time data. Fits were excellent, except for some experiments carried out at low denaturant concentrations which showed multiexponential kinetics. These experiments were not included in the chevron plots we report and analyze. Likewise, we do not include in the chevron plots the data at low denaturant concentration which show clear evidence of roll-over suggesting the occurrence of kinetic complications likely associated to proline isomerization and/or to the presence of kinetic intermediates. Therefore, we described our chevron plots on the basis of a two-state kinetic model:

$$\ln k = \ln(k_U + k_F) \tag{2}$$

where k_U and k_F are the unfolding and folding rate constants, which are assumed to change with denaturant concentration according to:

$$\ln k_F = \ln k_{1/2} + \frac{m_F}{RT}(C - C_{1/2}) \tag{3}$$

$$\ln k_U = \ln k_{1/2} + \frac{m_U}{RT}(C - C_{1/2}) \tag{4}$$

where m_F and m_U describe the urea-concentration effect on the activation free energies for folding and unfolding, respectively [$m_F = -(\partial \Delta G_{U\to\neq}/\partial C)$ and $m_U = -(\partial \Delta G_{N\to\neq}/\partial C)$, where $\neq$ stands for transition state] and $k_{1/2}$ is the value of both k_F and k_U at $C = C_{1/2}$. Equations (2)–(4) were found to describe adequately the chevron plots for all the thioredoxin variants studied in this work.

Global analysis of chevron plots obtained at different salt concentrations

The urea chevron plots at different salt concentrations were globally (i.e., simultaneously) fitted assuming that the kinetic m values were independent of salt concentration (global fits assuming linear dependencies of the kinetic m values with [NaCl] gave essentially the same results and very low values for the slopes of the assumed dependencies). In these fittings, m_U and m_F were used as global fitting parameters (i.e., they were taken to have the same values for all the chevron plots), while ln $k_{1/2}$ and $C_{1/2}$ were local parameters and were allowed to have different values for each chevron. Note that, for 1, 1.5, and 2*M* salt, the stability of the V6 variant is so high, that the midpoint urea concentration (approximately given by the "bottom" of the chevron plot) is not well defined in the experimental data. For 1 and 1.5*M* salt, we used as $C_{1/2}$ values in the global analysis, those directly obtained from equilibrium profiles derived from double-jump unfolding assays (see below). For 2*M* salt concentration, $C_{1/2}$ could not be determined from the double-jump unfolding assays (see below) and the corresponding chevron plot (which, in any case, would only show the folding branch) could not be included in the global analysis. Once the optimum values of the fitting parameters, values of the logarithms of folding and unfolding rate constants at [urea] = 7*M* and in the absence of denaturant, were calculated using Eqs. (3) and (4). The standard uncertainties associated to all values derived from the global fit were calculated using the method of

Bevington.[34] In the case of 2*M* salt concentration, the logarithm of the unfolding rate constant in the absence of urea was estimated from a linear plot of ln k_U([urea] = 0) versus equilibrium denaturation temperature including data for several salt concentrations (see supplementary Fig. 2S). Mutation effects on activation free energies were obtained on the basis of the transition-state relation $k = k_0 \exp(-\Delta G^{\neq}/RT)$ assuming that the front factor (k_0) is a constant.

Equilibrium denaturation profiles from double-jump unfolding assays

We have described the use of double-jump unfolding assays to determine chemical equilibrium denaturation profiles in several publications[20,35] and, therefore, only a brief account will be given here. The amount of protein present as native state under certain solvent conditions (denaturant concentration, for instance) can be determined from the unfolding kinetics observed upon transferring the protein to strongly denaturing conditions. In our unfolding assays, the protein was incubated in urea + salt solutions (Hepes 5 m*M*, pH 7) at 25°C for a time sufficient to guarantee that the unfolding equilibrium had been established and, subsequently, the unfolding kinetics was initiated by a several-fold dilution into high urea in 5 m*M* Hepes buffer, pH 7. Under these conditions the half-life for native-state denaturation is on the order of minutes. Unfolding kinetics were monitored by following the time-dependence of the fluorescence emission at 350 nm with excitation at 276 nm. Fluorescence intensity versus time profiles gave excellent fits to the first-order rate equation. The plot of amplitude of the fitted exponential (ΔI) versus urea concentration is the sought for equilibrium denaturation profile. Note that the analysis of this type of equilibrium profile is not complicated by pre- and post-transition baseline uncertainties, since ΔI approaches a constant value at low urea concentration and approaches zero at high urea concentration. Therefore, accurate values for the midpoint urea concentration can be obtained even when the equilibrium profile is not complete due to the high value of $C_{1/2}$ (see the profiles for 1 and 1.5*M* salt in supplementary Fig. 3S).

RESULTS AND DISCUSSION

Designing stabilizing mutations on the basis of sequence-alignment analysis

A number of studies have demonstrated statistical correlations between mutational effects on protein thermodynamic stability and the frequencies of occurrences of amino-acid residues in sequence alignments.[20,30,36–39] In fact, statistical analyses of sequence-alignments have been successfully used in some cases[8,9] to design modified proteins of enhanced stability ("consensus concept" to protein stabilization). In panel (A) of Figure 1, we show the results of a consensus analysis based on the sequences belonging to proteobacteria found in a BLAST search of the UniProt/TrEMBL database using the sequence of *E. coli* thioredoxin as query (see legend to Fig. 1 and Methods for details). We have determined, at each position, the amino-acid with the highest frequency of occurrence (consensus residue). In those cases in which the consensus residue differs from the residue in wt *E. coli* thioredoxin, the ratio of the corresponding frequencies of occurrence (consensus over wt) is shown. This ratio is particularly high for the wt to consensus mutations A22P, I23V, and P68A. We have, therefore, prepared the triple-mutant variant A22P/I23V/P68A, which will be subsequently referred to as the consensus variant or simply as V3. V3 shows indeed a much enhanced thermodynamic stability as reflected in an equilibrium denaturation temperature about 10° higher than that for the wt protein (Fig. 2).

We have recently proposed that statistical correlations between mutational effects on protein energetics and frequencies of amino-acid occurrences in sequence alignments reflect natural selection for kinetic stability (see Godoy-Ruiz *et al.*[20] for details). If this proposal is correct, we may expect that mutations suggested by the consensus concept occur in regions which are nonstructured in the transition state for unfolding, in such a way that the enhancement of thermodynamic stability is fully transmitted to the unfolding free-energy barrier and results in enhancement of kinetic stability. This is actually fulfilled by our consensus variant V3, as the kinetic chevron plots of Figure 3(A) clearly show. Note that the folding branches of the chevron plots for wt thioredoxin and the V3 variant agree, while there is a huge difference in the unfolding branches, indicating a several-orders-of-magnitude slower unfolding rate for the V3 variant as compared with WT. Note also that the chevron plots of Figure 3(A) have been obtained using guanidine as denaturant, since, due to its high stability, no significant unfolding of V3 in urea solutions is observed.

Designing destabilizing mutations on the basis of simple computational electrostatics

Panel (B) in Figure 1 shows the energies of charge–charge interactions for individual ionizable residues in the thioredoxin molecule, as calculated using a simple Tanford–Kirkwood model.[29] This is admittedly a very simple approach; nevertheless, it has been shown to qualitatively predict the effect of charge-deletion and charge-reversal mutations on the stability of several proteins and to account for the enhanced stability of cold-shock proteins from thermophilic and hyperthermophilic microorganisms.[2] Furthermore, charge–charge interaction

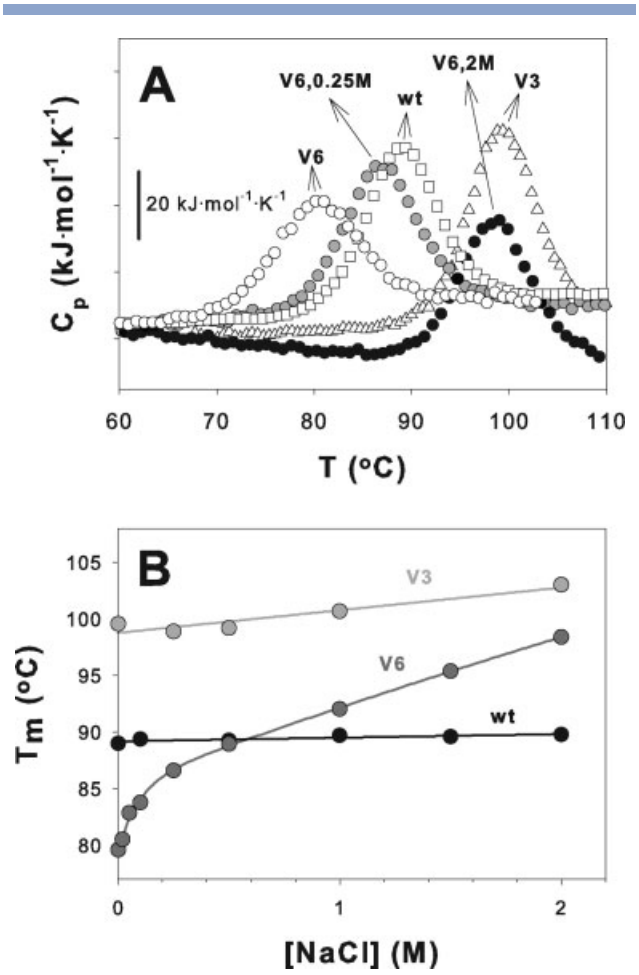

Figure 2

Salt effect on the thermodynamic stability of wt thioredoxin, the consensus (V3) and the consensus plus *charge-reversal (V6) variants. (**A**) Illustrative DSC profiles for the thermal denaturation of the three proteins. The profiles have been shifted in the y-axis for display purposes. For those experiments with salt added, the salt concentration is indicated alongside the variant name. (**B**) Effect of salt concentration on the equilibrium denaturation temperature for wt thioredoxin and the V3 and V6 variants.*

energies calculated with this simple Tanford–Kirkwood approach[29] have been shown[5] to be in reasonable agreement with those obtained using more rigorous methods (including finite-difference Poisson–Boltzmann).

In Figure 1(B), we give for each residue, the sum of the interaction energies with all other charged groups in the proteins. Positive values mean that the group is involved mainly in destabilizing charge–charge interactions with groups of the same charge. Likewise, negative values indicate that the group is involved in mainly stabilizing interactions with groups of the opposite charge. The pattern seen in Figure 1(B) (most energy values are negative) means that the surface charge distribution in wt thioredoxin is optimized to a significant extent, in such a way that most charged residues are surrounded by groups of the opposite charge. This type of optimized surface charge distribution is actually quite common among proteins, as Wada and Nakamura[40] noted more than 25 years ago. In this situation, few stabilizing single charge-reversal mutations can be found, but there are plenty of choices for destabilizing charge reversal mutations. In fact, it appears plausible that, for proteins of unknown 3D structure, the design of destabilizing charge-interactions could be easily carried out on the basis of a simple screening of the effects of charge-reversal mutations. Nevertheless, knowledge of the 3D structure, together with the use of a suitable electrostatic model, should certainly focus the screening procedure. Thus, visual inspection of Figure 1(B) suggests positions 3, 18, 69

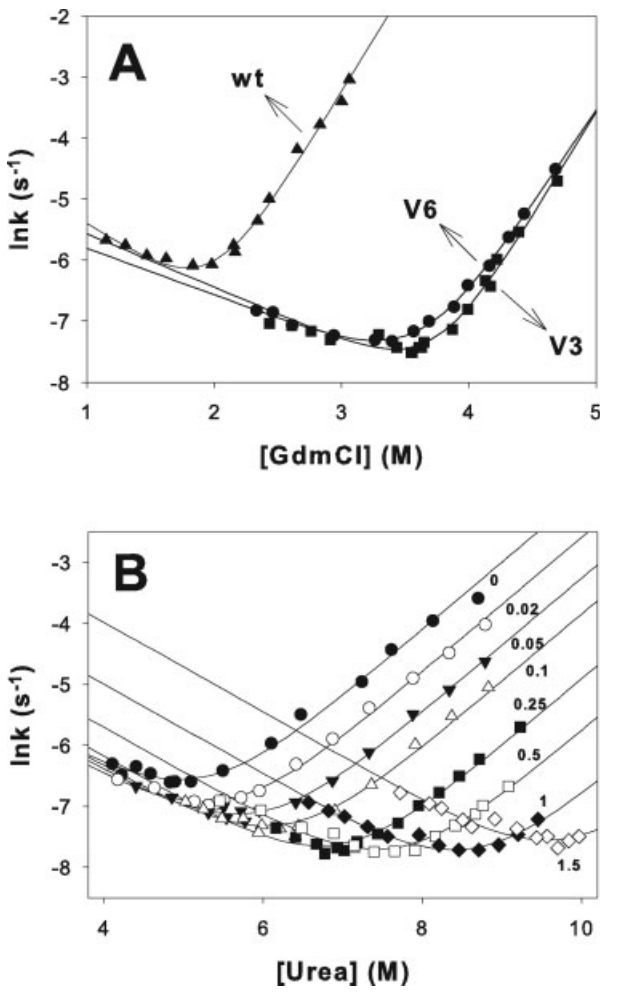

Figure 3

*Folding–unfolding kinetics for thioredoxin. (**A**) Guanidine chevron plots for wt thioredoxin and the V3 and V6 variants. The lines are the best fits of Eqs. (1)–(3). (**B**) Urea chevron plots for the consensus* plus *charge-reversal, V6 variant. The numbers alongside the plots stand for the salt concentration. The lines are the best global fit of Eqs. (2)–(4) to all the chevron plots, assuming that the kinetic-m values do not depend on salt concentration.*

and 96 as more promising in the case of E. coli thioredoxin and lysine to glutamate mutations at those positions should introduce interactions between groups of negative charge which will be destabilizing, but easily screened by salt.

In a first step, we prepared four single mutants of wt thioredoxin with the K3E, K18E, K69E, and K96E mutations. We found them to be significantly less stable than wt at low salt but to be strongly stabilized by increasing salt concentration (see supplementary Fig. 4S), with the exception of the K96E variant, possibly due to the formation of a salt bridge between the glutamate introduced at position 96 and K100. In a second step, we introduced the three destabilizing charge-reversal mutations in the stabilized consensus V3 variant (attempts to introduce the three charge-reversal mutations in the wt protein were unsuccessful, possibly due to very low protein stability). The resulting sixfold-mutant variant (K3E/K18E/A22P/I23V/P68A/K69E) will be subsequently referred to as the consensus *plus* charge-reversal variant or, simply, as V6. V6 shows at low salt (but not at high-salt!) a much decreased stability with respect to V3 and even with respect to wt thioredoxin (see next section).

It should be noted that the charge-reversal mutations are introduced at surface positions which may be reasonably presumed to be outside any "folding nucleus" (or structured region) in the folding/unfolding transition state. Accordingly, we may expect that the effects of these mutations on the unfolding free-energy change will be transmitted to a large extent to the unfolding free-energy barrier. This expectation is actually confirmed by the experimental results we describe further below and by the fact that there is only a comparatively small difference between the folding branches of the urea–chevron plots for wt thioredoxin and the V6 variant agree, while there is a very large difference in the unfolding branches (see supplementary Fig. 5S).

Salt effects on thermodynamic stability

Figure 2(B) shows the effect of salt (NaCl) concentration on the equilibrium denaturation temperature (T_m) values for wt thioredoxin, the consensus V3 variant and the consensus + charge-reversal (V6) variant. The T_m values are derived from equilibrium DSC experiments [see Methods for details and Fig. 2(A) for illustrative DSC profiles]. Only small dependencies of the equilibrium denaturation temperature with salt concentration are found for wt thioredoxin and the V3 variant. By contrast, a huge salt effect is found for the V6 variant, which shows a T_m value about ten degrees below that of wt thioredoxin and a T_m value approaching that of the V3 variant at high salt, indicating that the destabilizing interactions between negative charges introduced in the V6 variant are to a large extent screened out at 1.5–2*M* salt. [This is further supported by the good agreement between the guanidine chevron plots for V3 and V6 [Fig. 3(A)]; note that guanidine is a salt and screens efficiently charge–charge interactions]. Note that there is a large difference (about 20°) between the T_m values of V6 at low- and high-salt.

Salt effects on folding/unfolding kinetics

V6 shows enhanced thermodynamic stability with respect to wt at high salt, and decreased thermodynamic stability at low-salt [Fig. 2(B)], which is exactly the behavior we intended to achieve. In order to ascertain to what extent this thermodynamic behavior is reflected in kinetics, we have determined the kinetic chevron plots in the presence of different salt concentrations and using urea as denaturant. For the consensus *plus* charge-reversal V6 variant, a huge salt effect is observed [Fig. 3(B) and supplementary Fig. 6S]. Furthermore, a simple visual inspection indicates that the large effect is mostly centered upon the unfolding branches, with the folding branches showing only a moderate change above 0.5*M* salt.

In order to quantify the above observation, we have performed a global analysis of the chevron plots of Figure 3(B) assuming that the kinetic *m* values do not depend on salt concentration (see Methods for details). Some results of the global analysis are given in Figure 4 (see also supplementary Table 1), where a strong decrease in unfolding rate constants with salt concentration is apparent.

We show in Figure 5 a plot of the salt effect on unfolding activation free-energy (activation ΔG at a given salt concentration minus activation ΔG in the absence of salt) versus the salt effect on equilibrium free-energy change (equilibrium ΔG at a given salt concentration minus equilibrium ΔG in the absence of salt). If the salt effects on equilibrium ΔG were fully transmitted to the unfolding barrier, this plot would yield a straight line with slope equal to 1. In fact, the plot of Figure 5 shows a small but significant curvature, although it does not depart much from the straight line of unity slope. The derivative of the plot ($\phi_{NaCl} = d\Delta\Delta G^{\neq}/d\Delta\Delta G$) should provide a measure of the fraction of the salt effect on equilibrium ΔG which is "transmitted" to the unfolding barrier. ϕ_{NaCl} is close to unity at low salt (see inset in Fig. 5) but decreases somewhat at high-salt. This decrease may reflect that the salt-dependencies at the higher salt concentrations are determined, not only by charge-screening, but also by general solvent effects which are likely to be related to the overall exposure to solvent in the states involved (native, unfolded, and transition state). Note that the exposure to solvent in the transition state is expected to be intermediate between those of the native and unfolded states. Consequently, general solvent effects on activation free-energy are expected to be smaller than those on unfolding free-energy. In any case,

the results shown in Figure 5 are qualitatively consistent with the charge-reversal mutations (K3E, K18E, and K69E) being in regions which are mostly nonstructured in the unfolding transition state, which, as a result, lacks the salt-screenable interactions between like-charges present in the native state of V6.

Salt effects on the time-scale associated to the unfolding barrier

The global analysis of the data in Figure 3(B) (see Methods for details) allows us to obtain values for the unfolding rate constants at zero denaturant concentration (see Fig. 4). This certainly involves a rather long extrapolation based on a linear dependence of the free-energy changes with denaturant concentration. However, deviations from such linear dependencies have been reported to be small in the case of urea.[41] Furthermore, the results obtained (see Fig. 4) reveal a several orders-of-magnitude change in time-scale, a robust feature which will be essentially unaffected by any uncertainties of the extrapolation procedure. Note, in fact, that the unfolding half-life time in the absence of denaturant changes from being of the order of a few days at low salt to being of the order of many years at high-salt. We emphasize again that this unfolding half-life times will set the time-scales for irreversible denaturation process that are limited by the "crossing" of the unfolding barrier. Therefore, these results highlight the possibility of engineering proteins with strongly environment-dependent kinetic stability.

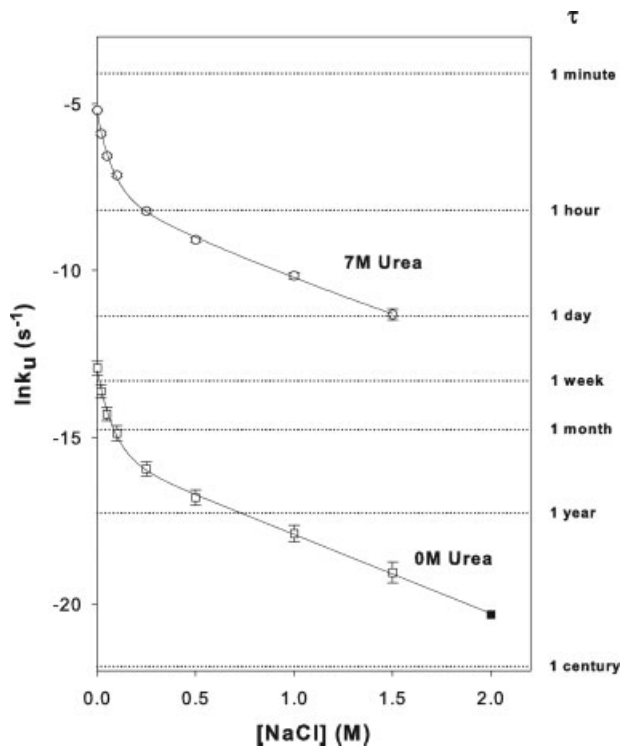

Figure 4

Effect of salt on the unfolding rates for the consensus plus *charge-reversal variant (V6) of thioredoxin at 7M urea and in the absence of denaturant (0M urea). The values were derived from the global fit shown in Figure 3(B), except for the value at 2M salt, which is obtained from the empirical linear relation between logarithm of unfolding rate constant and the equilibrium denaturation temperature (see supplementary Fig. 2S). Error bars are the associated uncertainties calculated using Bevington's method. The right axis indicates the rate constant values corresponding to representative half-life times.*

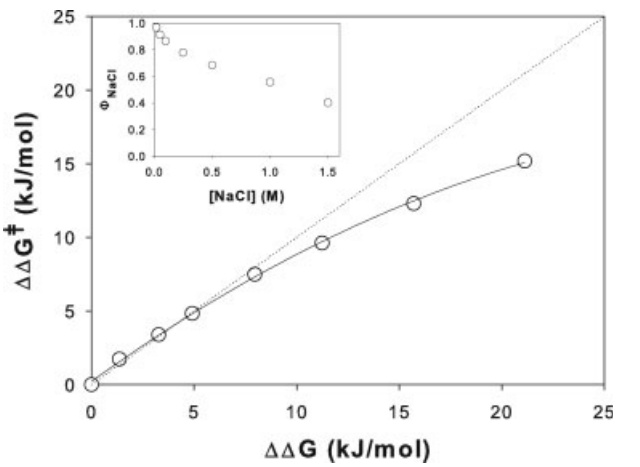

Figure 5

Effect of salt on the activation free-energy for unfolding versus the effect of salt on the equilibrium free-energy change, for the consensus plus *charge-reversal variant (V6). In each case, the ΔΔG values given are the differences between ΔG (activation or equilibrium) at a given salt concentration and ΔG in the absence of added salt. The dotted straight line has slope equal to unity. The continuous line is the best fit of a second-order polynomial. The values of the derivative of the fitted polynomial are plotted versus salt concentration in the Inset.*

CONCLUDING REMARKS

We have shown that strong environment-dependencies of protein thermodynamic and kinetic stabilities can be easily achieved and, as a result, that enhanced stability or decreased stability (with respect to wt) may be realized depending on the solvent conditions. We have demonstrated this possibility using a two-state protein system as a model. However, the design approaches we have employed here should also lead to strongly environment-dependent kinetic stabilities for non-two-state proteins, provided that the kinetically-relevant transition states are targeted. This will, of course, require "structural pictures" of those transition states, in such a way that mutations can be introduced in nonstructured regions. Recent success in the enhancement of the kinetic stability[15] of a lipase (an important industrial enzyme) suggests that molecular dynamics simulations may be useful in determining such nonstructured regions.

The specific design procedures we have followed involve stabilizing consensus mutations and destabilizing electrostatic mutations, the latter introducing salt-screenable interactions between like charges. However, our general approach could be implemented in different ways as required. For instance, the stabilization step could be carried out on the basis of rational/computational methods,[1,4] provided that mutations are introduced in regions which are nonstructured in the unfolding transition state and that, consequently, thermodynamic stabilization translates into enhancement of kinetic stability; such regions could in principle be located by classic ϕ-value analysis or, possibly, by molecular dynamics simulations.[15] In addition, the fact that many charged residues in native proteins participate in stabilizing interactions with residues of opposite charge[40] implies that, in most cases, several possibilities for the electrostatic destabilization step (i.e., several choices for the set of destabilizing charge-reversal mutations) should be available. For the same reason, the electrostatic destabilization step is expected to be robust and the choice of electrostatic model (we have used a simple Tanford–Kirkwood calculation) should not be critical here. Overall, it appears likely that, for a given protein, several different variants with strongly environment-dependent thermodynamic and kinetic stabilities can be designed and obtained along the general lines described in this work. This should facilitate the optimization or fine-tuning with respect to other features (function, pharmacokinetics, etc.).

Finally, it must be noted that very large changes in salt concentration are not expected to occur in biological systems *in vivo*. Strong salt-dependencies of the thermodynamic and kinetic stabilities of proteins are more likely to be useful in those cases in which high-stability is required only under storage conditions. A plausible scenario is that inclusion of high salt in liquid formulations will contribute to a long protein shelf-life, while the lower salt concentration under the conditions of the application will help prevent the side effects associated with high-stability which may potentially arise in some therapeutic and food-industry applications. From a more general viewpoint, this work shows that consensus engineering and electrostatic engineering can be readily combined and clarifies relevant aspects of the relation between thermodynamic stability and kinetic stability in proteins.

REFERENCES

1. Malaskauskas SM, Mayo SL. Design, structure and stability of a hyperthermophilic protein variant. Nat Struct Biol 1998;5:470–475.
2. Sanchez-Ruiz JM, Makhatadze GI. To charge or not to charge? Trends Biotechnol 2001;19:132–135.
3. Ibarra-Molero B, Sanchez-Ruiz JM. Genetic algorithm to design stabilizing surface-charge distributions in proteins. J Phys Chem B 2002;106:6609–6613.
4. Korkegian A, Black ME, Baker D, Stoddard BL. Computational thermostabilization of an enzyme. Science 2005;308:857–860.
5. Strickler SS, Gribenko AV, Gribenko AV, Keiffer TR, Tomlinson J, Reihle T, Loladze VV, Makhatadze GI. Protein stability and surface electrostatics: a charged relationship. Biochemistry 2006;45:2761–2766.
6. Perl D, Mueller U, Heinemann U, Schmid FX. Two exposed amino acid residues confer thermostability on a cold shock protein. Nat Struct Biol 2000;7:380–383.
7. Pace CN. Single surface stabilizer. Nat Struc Biol 2000;7:345–346.
8. Lehman M, Pasamontes L, Lassen SF, Wyss M. The consensus concept for thermostability engineering of proteins. Biochim Biophys Acta 2000;1543:408–415.
9. Steipe B. Consensus-based engineering of protein stability: from intrabodies to thermostable enzymes. Methods Enzymol 2004;388:176–186.
10. Eijsink VG, Gaseidnes S, Borchert TV, van der Burg B. Directed evolution of enzyme stability. Biomol Eng 2005;22:21–30.
11. Leland PA, Raines RT. Cancer chemotherapy—ribonucleases to the rescue. Chem Biol 2000;8:405–413.
12. Vasandani VM, Wu YN, Mikulski SM, Youle RJ, Sung C. Molecular determinants in the plasma clearance and tissue distribution of ribonucleases of the ribonuclease A superfamily Cancer Res 1996;56:4180–4186.
13. Vasandani VM, Burris JA, Sung C. Reversible nephrotoxicity of onconase and effect of lysine pH on renal onconase uptake. Cancer Chemoter Pharmacol 1999;44;164–169.
14. Notomista E, Catanzano F, Graziano G, Dal Piaz F, Barone G, D'Alessio G, Di Donato A. Onconase: an unusually stable protein. Biochemistry 2000;39:8711–8717.
15. Rodríguez-Larrea D, Minning S, Borchert TV, Sanchez-Ruiz JM. Role of solvation barriers in protein kinetic stability. J Mol Biol 2006;360:715–724.
16. Plaza del Pino IM, Ibarra-Molero B, Sanchez-Ruiz JM. Lower kinetic limit to protein termal stability: a proposal regarding protein stability in vivo and its relation with misfolding diseases. Proteins: Struct Funct Genet 2000;40:58–70.
17. Lumry R, Eyring H. Conformational changes in proteins. J Phys Chem 1954;58:110–120.
18. Klibanov AM, Ahern TJ. Thermal stability of proteins. In: Oxender DL, Fox CF, editors. Protein engineering. New York: Liss; 1987. pp 213–218.
19. Sanchez-Ruiz JM. Theoretical analysis of Lumry–Eyring models in differential scanning calorimetry. Biophys J 1992;61:921–935.
20. Godoy-Ruiz R, Ariza F, Rodríguez-Larrea D, Perez-Jimenez R, Ibarra-Molero B, Sanchez-Ruiz JM. Natural selection for kinetic stability is a likely origin of correlations between mutational effects on protein energetics and frequencies of amino acid occurrences in sequence alignments. J Mol Biol 2006;362:966–978.
21. Gruebele M. Downhill protein folding: evolution meets physics. C R Biol 2005;328:701–712.
22. Dobson CM. Protein misfolding, evolution and disease. Trends Biochem Sci 1999;24:329–332.
23. Jaenicke R, Böhm G. The stability of proteins in extreme environments. Curr Opin Struct Biol 1998;8:738–748.
24. Jaenicke R. Do ultrastable proteins from hyperthermophiles have high or low conformational rigidity? Proc Natl Acad Sci USA 2000;97:2962–2964.
25. Zeeb M, Lipps G, Lilie H, Balbach J. Folding and association of an extremely stable dimeric protein from *Sulfolobus islandicus*. J Mol Biol 2004;336:227–240.
26. Sohl JL, Jaswal SS, Agard DA. Unfolded conformations of alphalytic protease are more stable than its native state. Nature 1998;395:817–819.
27. Park C, Zhou S, Gilmore J, Marqusee S. Energetics-based profiling on a proteomic scale: identification of proteins resistant to proteolysis. J Mol Biol 2007; doi: 10.1016/j.jmb.2007.02.091.
28. Godoy-Ruiz R, Perez-Jimenez R, Ibarra-Molero B, Sanchez-Ruiz JM. A stability pattern of protein hydrophobic mutations that

reflects evolutionary structural optimization. Biophys J 2005; 89:3320–3331.
29. Ibarra-Molero B, Loladze VV, Makhatadze GI, Sanchez-Ruiz JM. Thermal versus guanidine-induced unfolding of ubiquitin. An analysis in terms of the contributions from charge–charge interactions to protein stability. Biochemistry 1999;38:8138–8149.
30. Godoy-Ruiz R, Perez-Jimenez R, Ibarra-Molero B, Sanchez-Ruiz JM. Relation between protein stability, evolution and structure, as probed by carboxylic acid mutations. J Mol Biol 2004;336:313–318.
31. Perez-Jimenez R, Godoy-Ruiz R, Ibarra-Molero B, Sanchez-Ruiz JM. The efficiency of different salts to screen charge interactions in proteins: a Hofmeister effect? Biophys J 2005;35:14689–14702.
32. Holmgren A. Thioredoxin catalyzes the reduction of insulin disulfides by dithiothreitol and dihydrolipoamide. J Biol Chem 1979; 254:9627–9632.
33. Slaby I, Holmgren A. Structure and enzymatic functions of thioredoxin refolded by complementation of two tryptic peptide fragments. Biochemistry 1979;18:5584–5591.
34. Bevington PR. Data Reduction and Error Analysis for the Physical Sciences. New York: McGraw-Hill; 1969. 336 p.
35. Ibarra-Molero B, Sanchez-Ruiz JM. A model-independent, nonlinear extrapolation procedure for the characterization of protein folding energetics from solvent-denaturation data. Biochemistry 1996; 35:14689–14702.
36. Campos LA, Garcia-Mira MM, Godoy-Ruiz R, Sanchez-Ruiz JM, Sancho J. Do proteins always benefit from a stability increase? Relevant and residual stabilisation in a three-state protein by charge optimization. J Mol Biol 2004;344:223–237.
37. Steipe B, Schiller B, Plückthun A, Steinbacher S. Sequence statistics reliably predicts stabilizing mutations in a protein domain. J Mol Biol 1994;240:182–192.
38. Pielak GJ, Auld DS, Beasley JR, Betz SF, Cohen DS, Doyle DF, Finger SA, Fredericks ZL, Hilgen-Willis S, Saunders AJ, Trojak SK. Protein thermal denaturation, side-chain models, and evolution: amino acid substitutions at a conserved helix–helix interface. Biochemistry 1995;34:3268–3276.
39. Sanchez IE, Tejero J, Gomez-Moreno C, Medina M, Serrano L. Point mutations in protein globular domains: contributions from function, stability and misfolding. J Mol Biol 2006;363:422–432.
40. Wada A, Nakamura H. Nature of the charge distribution in proteins. Nature 1981;293:757–758.
41. Ibarra-Molero B, Perez-Jimenez R, Godoy-Ruiz R, Sanchez-Ruiz JM. In: Ladbury JE, Doyle ML, editors. Biocalorimetry 2. Applications of calorimetry in the biological sciences. Chichester: Wiley; 2004. pp 201–214.